
LATTICE DYNAMICS AND PHASE TRANSITIONS

Phase Transitions in Oxyfluoride $(\text{NH}_4)_2\text{WO}_2\text{F}_4$

S. V. Mel'nikova*, V. D. Fokina*, and N. M. Laptash**

*Kirensky Institute of Physics, Siberian Division, Russian Academy of Sciences,
Akademgorodok, Krasnoyarsk, 660036 Russia

e-mail: msv@iph.krasn.ru

**Institute of Chemistry, Far East Division, Russian Academy of Sciences,
pr. Stoletiya Vladivostoka 159, Vladivostok, 690022 Russia

Received February 3, 2005; in final form, April 18, 2005

Abstract— $(\text{NH}_4)_2\text{WO}_2\text{F}_4$ single crystals are grown, and their polarization-optical, calorimetric, and birefringence properties are studied in the temperature range 90–350 K. A first-order structural phase transition is found to occur at $T_{01\uparrow} = 202$ K with thermal hysteresis of $\Delta T_{01} \approx 6$ –12 K. The phase transition is accompanied by twinning and modification of the symmetry $Cmcm \longleftrightarrow \bar{1}$. An additional weak anomaly in the differential scanning calorimeter signal is found at $T_{02} \approx 170$ K. The total thermal effect of both anomalies is $\sum \Delta H_i = 3200 \pm 400$ J/mol and $\sum \Delta S_i = 16.5 \pm 2.0$ J/mol K. The phase transition at T_{01} is of the order–disorder type.

PACS numbers: 64.70.Kb, 65.40.Ba, 78.20.Fm

DOI: 10.1134/S1063783406010239

1. INTRODUCTION

Oxyfluoride compounds $A_2\text{MO}_2\text{F}_4$ ($A = \text{Na}, \text{Rb}, \text{Cs}$, or a molecular cation; $M = \text{W}, \text{Mo}$) have been actively studied by various physical methods for a number of years [1–7]. The interest in these compounds is great because they promise to provide new materials with a wide transparency range without an inversion center, because their lattice consists of cations A and isolated polar octahedral groups $\text{MO}_2\text{F}_4^{2-}$.

However, most of these compounds crystallize in centrosymmetric structures because their building blocks are orientationally disordered. So, in order to produce the desired result, it is necessary to determine the reason behind the orientation disorder of oxyfluoride anions.

Depending on the size and shape of the A cations, lattices of different symmetries and different degrees of ordering of the ion groups $\text{MO}_2\text{F}_4^{2-}$ can form in the family under study. Polar symmetry has been successfully produced in compounds with two different multiatomic organic cations [5–7]. The lattice of $\text{Cs}_2\text{WO}_2\text{F}_4$ ($P\bar{3}m1$) is completely disordered with respect to oxygen and fluoride [3], $\text{Rb}_2\text{MoO}_2\text{F}_4$ ($Cmcm$) is partly ordered [1], and in $\text{Na}_2\text{WO}_2\text{F}_4$ ($Pbcn$) the ligand atoms are completely ordered [2]. So far, there have been no studies on the thermal stability of these phases, let alone on variation of the ligand ordering as a result of phase transitions in the $A_2\text{MO}_2\text{F}_4$ compounds, and, as

far as we know, there is no published data on the structural changes occurring in them.

According to [8], a $(\text{NH}_4)_2\text{WO}_2\text{F}_4$ crystal is partly ordered at room temperature; its symmetry is $Cmcm$ ($Z = 4$); and its lattice constants are $a = 5.9510$ Å, $b = 14.441$ Å, and $c = 7.1571$ Å.

In the present work, polarization-optical studies and measurements of the heat capacity and birefringence of $(\text{NH}_4)_2\text{WO}_2\text{F}_4$ crystals are carried out in a wide temperature range in order to detect phase transitions and perform a preliminary study of them.

Heat capacity studies were performed using a DSM-2M differential scanning microcalorimeter (DSM) in the temperature range 120–370 K. Measurements were performed under heating and cooling at a scanning rate of 8 K/min. To increase the reliability of the results, the experiments were conducted on a series of samples grown in different batches. The weights of samples ranged from 0.15 to 0.20 g. The birefringence was studied on (001)-, (010)-, and (100)-cut plates using the Berek compensator method with a precision of $\approx 10^{-5}$ and the Senarmont compensator method with a sensitivity of at least $\approx 10^{-7}$ at a wavelength of 6328 Å. The former method was employed to obtain the absolute value of the birefringence, and the latter was used to study its temperature dependence. The polarization-optical observations were performed using an AxioLab polarization microscope. All measurements were carried out in the temperature range from 90 to 350 K.

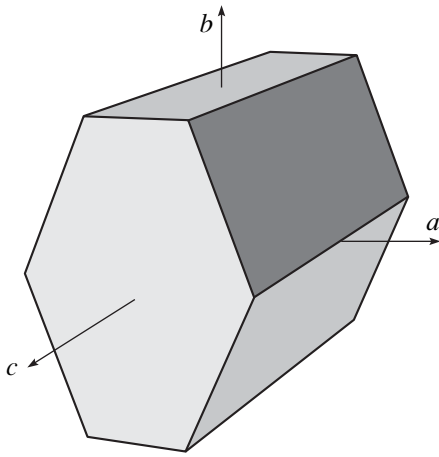


Fig. 1. Habitus of $(\text{NH}_4)_2\text{WO}_2\text{F}_4$ crystals.

2. EXPERIMENTAL RESULTS

Clear transparent $(\text{NH}_4)_2\text{WO}_2\text{F}_4$ single crystals up to 0.5 cm^3 in volume were grown by slow evaporation of a saturated fluoride water solution of a salt obtained either as a product of the reaction of ammonium paratungstate and concentrated HF (40 wt %) or by fluorination of CaWO_4 by NH_4HF_2 at 473 K and subsequent leaching of the cake by water. At first glance, the crystals grown have different shapes: hexagon plates or elongated rectangles. However, a close inspection reveals that the crystals are hexagonal prisms with angles of 136° and 112° between the faces (Fig. 1), complying with the ratio of the lattice constants a/b .

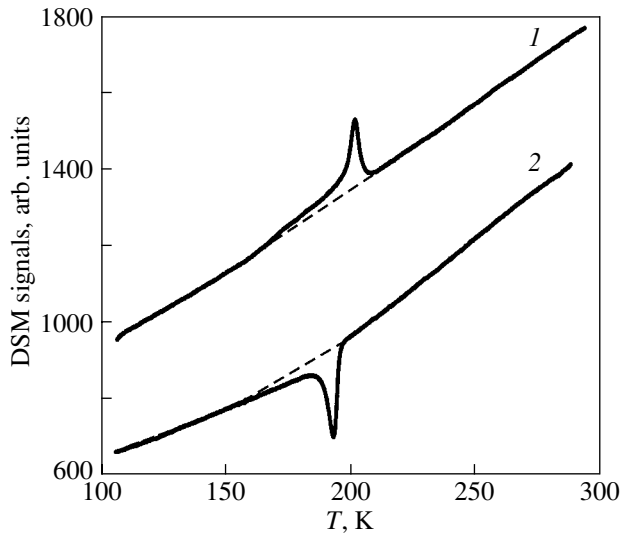


Fig. 2. Temperature dependence of the DSM signal during (1) heating and (2) cooling. Dashed lines show the polynomial fit for the regular contribution to the signal calculated beyond the anomalous region.

Investigations of $(\text{NH}_4)_2\text{WO}_2\text{F}_4$ plates cut along the principal crystallographic orientation performed in polarized light at room temperature revealed a smooth parallel extinction typical of orthorhombic crystals. The shape of the optical indicatrix corresponds to an optical negative crystal. Above room temperature, in the (001) cut, we observe an acute bisectrix with the (010) optic axial plane and the following refraction indices: $n_c = n_p$, $n_a = n_g$, and $n_b = n_m$. Below room temperature, the orientation of the optic axial plane changes to (100): $n_c = n_p$, $n_a = n_m$, and $n_b = n_g$.

The temperature dependences of the DSM signal obtained during a thermal cycle are shown in Fig. 2. On heating, we observe a signal anomaly (a sharp peak with a maximum at $T_{01} = 202 \pm 1 \text{ K}$), which is evidence of a phase transition occurring in $(\text{NH}_4)_2\text{WO}_2\text{F}_4$ at this temperature. Cooling reveals hysteresis of the transition temperature $\delta T_{01} = 9 \pm 1 \text{ K}$. In addition to this peak, the DSM signal curve obtained under heating contains another weak anomaly near the temperature $T_{02} = 170 \text{ K}$. The existence of both anomalies is confirmed by multiple measurements on six different samples.

The temperature dependences of the birefringence Δn_a , Δn_b , and Δn_c of $(\text{NH}_4)_2\text{WO}_2\text{F}_4$ crystals are shown in Fig. 3. At room temperature, the values of birefringence in the [100] (Δn_a) and [010] (Δn_b) directions are roughly the same (≈ 0.02) and the value of Δn_c in the [001] direction is almost zero.

For the (001) cut, we observed the optical-isotropy point at a wavelength $\lambda = 6328 \text{ \AA}$ at $T = 284 \text{ K}$. Further heating or cooling causes the birefringence to change sign. The temperature dependence of the birefringence on cooling in the range 350–260 K is linear and below

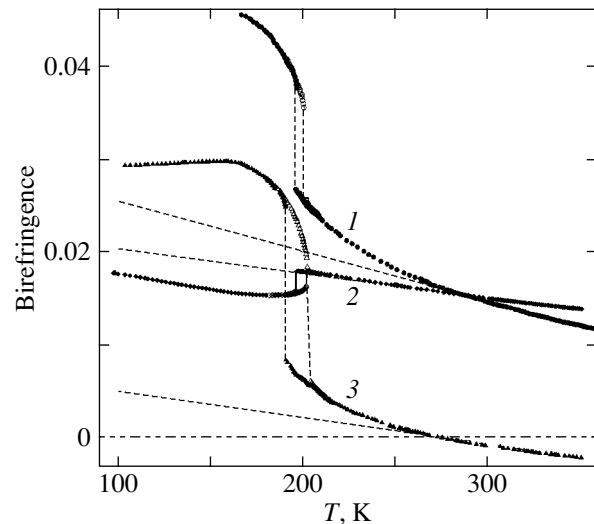


Fig. 3. Temperature dependence of the birefringence of $(\text{NH}_4)_2\text{WO}_2\text{F}_4$: (1) Δn_a , (2) Δn_b , and (3) Δn_c .

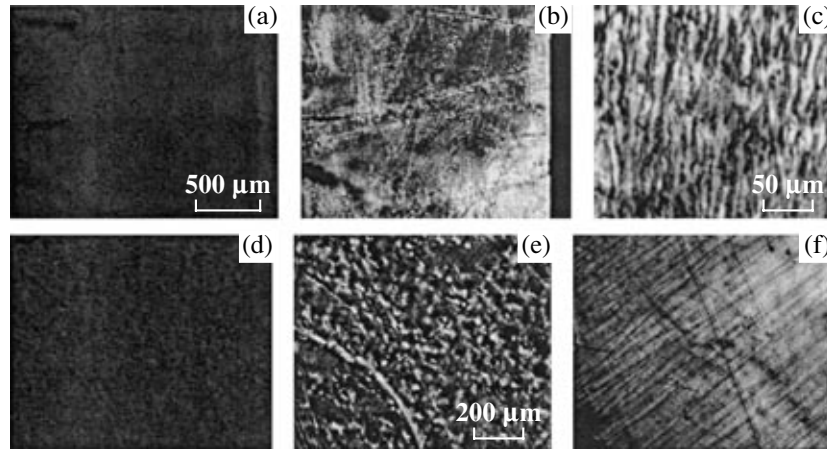


Fig. 4. Extinction of $(\text{NH}_4)_2\text{WO}_2\text{F}_4$ crystal plates in polarized light for (a, b) thick (100)-cut samples at the extinction angle above and below the phase transition point, respectively; (c) a thin (100)-cut sample at $T = 150$ K; (d) good extinction of thin (010) and (001) cuts at 150 K; and (e, f) visualization of a twin structure at a small angle ($\pm\phi \approx 1^\circ\text{--}2^\circ$) away from the extinction positions for (e) thin (010)-cut sample and (f) thin (001)-cut sample.

this range deviates from linearity in the (100) and (001) cuts. In Fig. 3, the extrapolated straight lines of the birefringence temperature dependences are shown by dashed lines. It can be seen that, in the crystal under study, there is a ≈ 70 -K-wide temperature range above the phase transition where strong precursor phenomena occur. Below ≈ 200 K, there occurs a phase transition, which is accompanied by a jump in birefringence and by thermal hysteresis, the magnitude of which varies from one experiment to another (Fig. 3). The phase transition point as observed on cooling varies in position in the range $T_{01\downarrow} = 190\text{--}196$ K depending on the sample. The phase transition point observed on heating is always the same, $T_{01\uparrow} = 202$ K; therefore, the thermal hysteresis is different, $\delta T_{01} \approx 6\text{--}12$ K, in different experiments. Some cracks arise in the samples during the phase transition. There is a small inflection in the $\Delta n_c(T)$ curve near the temperature $T_2 \approx 170$ K. Measurements of $\Delta n_c(T)$ were performed only above this temperature because of strong light scattering.

Studying crystal samples ~ 1 - to 2-mm thick in polarized light showed that, in the entire temperature range covered, the extinction for the (010) and (001) cuts remain even, without any twinning. The (100) cut also exhibits a good extinction (Fig. 4a); however, below $T \approx 200$ K, its clearness deteriorates gradually and grains appear. On further cooling, the contrast of the image grows, spots become colored, but no regular structure is visible (Fig. 4b). On heating, the sequence repeats itself with a thermal hysteresis.

A somewhat different situation is observed below T_{01} for thin (~ 100 - μm -thick) plates. We managed to record a fine needlelike systematic structure in the (100) cut at high magnification (Fig. 4c), in which there were components differing in terms of the extinction angles; the difference in angle is relatively large, $2\phi \approx$

$10^\circ\text{--}14^\circ$. In the cuts where a clear extinction is observed for thick samples, the extinction is also good for thin samples (Fig. 4d). However, at small deviations from the extinction angle, a very weak “flickering” twin structure is observed with very small misorientation angles of the optical indicatrices, $2\phi \approx 2^\circ\text{--}3^\circ$. In the (010) cut, the structure has the form of alternating dark and light blots (Fig. 4e), and, in the (001) cut, the structure looks like a system of wedgelike bands (Fig. 4f).

No changes in extinction for plates of any cut are found around $T_2 \approx 170$ K. The results described above are not affected significantly when a compressive stress X_4 is applied. We also did not observe optical second-harmonic generation in the temperature range indicated above.

3. DISCUSSION

The results of our experiments indicate that a phase transition occurs in $(\text{NH}_4)_2\text{WO}_2\text{F}_4$ crystals at $T_{01\uparrow} = 202$ K. The phase transition is accompanied by a thermal anomaly, a jump in the birefringence, and a thermal hysteresis typical of first-order transitions. According to the observations in polarized light, the high-temperature phase has orthorhombic symmetry. The visualization of the fine twin structure at $T < T_{01}$ in all three orthogonal directions and misorientation of the optical indicatrices of adjacent twins indicate that all symmetry planes and twofold symmetry axes existing in the crystal at room temperature are lost as a result of the phase transition. The absence of optical second-harmonic generation at low temperatures indicates that there is a center of symmetry and that a first-order phase transition occurs at $T_{01} \approx 202$ K with a change in symmetry $Cmcm \longleftrightarrow \bar{1}$. The optical inhomogeneities observed in relatively thick samples below the phase

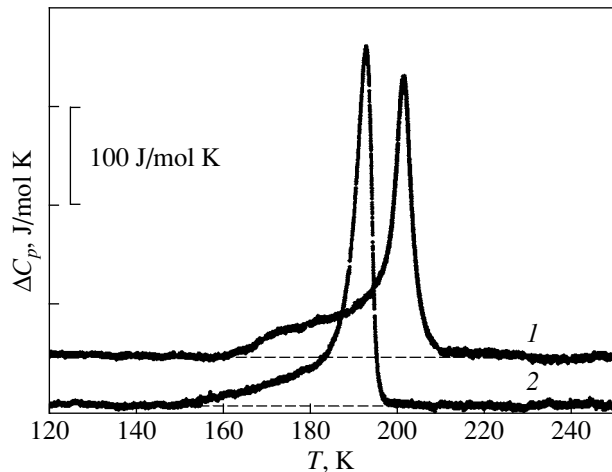


Fig. 5. Temperature dependence of the anomalous specific heat of $(\text{NH}_4)_2\text{WO}_2\text{F}_4$ during (1) heating and (2) cooling.

transition are the integrated optical effect of the fine twin structure.

Our attempts to detect structural changes below T_{01} using x-ray powder diffraction failed; we found no discernible differences in the diffraction patterns between the high- and low-temperature phases at 290 and 120 K, respectively. Thus, we can assume that, in spite of the pronounced first-order phase transition at T_{01} and substantial changes in the birefringence and symmetry, the orthorhombic unit cell of the $(\text{NH}_4)_2\text{WO}_2\text{F}_4$ crystal is distorted only slightly in the phase transition.

Optical studies provided no proof of a change in the symmetry at $T = T_2$. However, all the results obtained suggest that the oxyfluoride under study undergoes a sequence of two phase transitions at T_{01} and T_{02} .

In order to isolate the anomalous contribution to the heat capacity associated with the phase transition, we make a polynomial fit to the portions of the DSM-signal curve far away from the temperatures T_{01} and T_{02} (Fig. 2). The anomalous contribution was determined by subtracting the regular contribution from the total DSM signal, and then the temperature dependence of the heat capacity was found using the heat capacity data for corundum as a reference. In this way, we determined the temperature dependence of the excess specific heat ΔC_p of the $(\text{NH}_4)_2\text{WO}_2\text{F}_4$ crystal (Fig. 5).

Presented this way, the low-temperature anomaly is more pronounced, though only on the heating curve. The fact that the anomalous behavior of ΔC_p around $T_{02\downarrow}$ is less prominent on cooling may be due to the considerable difference in the hysteresis magnitude between the two phase transitions, which can lead to merging of the heat capacity anomalies.

Using the heat capacity measurements, we determined the integrated characteristics of the phase transitions in $(\text{NH}_4)_2\text{WO}_2\text{F}_4$. The changes in enthalpy (ΔH)

and in entropy (ΔS) are found by integrating $\Delta C_p(T)$ and $(\Delta C_p/T)(T)$, respectively, over the temperature. In this stage of investigation, we cannot separate the anomalous contributions from each of the phase transitions to the heat capacity. Therefore, we give only the total values: $\sum \Delta H_i = 3200 \pm 400$ J/mol and $\sum \Delta S_i = 16.5 \pm 2.0$ J/mol K. From the temperature dependence of the excess heat capacity (Fig. 5), it follows that the overwhelming contribution to $\sum \Delta S_i$ comes from the change in entropy at T_{01} . This means that at least this phase transition can be attributed to the order–disorder type, since the value $\sum \Delta S_i = 1.98R = R \ln 7.3$ clearly indicates disordering of some building blocks in the orthorhombic phase. The strong precursor birefringence tails, which are up to 30% of the jump at the transition point (Fig. 3), are also typical of order–disorder transitions.

According to [8], the lattice of $(\text{NH}_4)_2\text{WO}_2\text{F}_4$ consists of ammonium cations (tetrahedra) and isolated octahedra. These building blocks often play a critical role, because their ordering distorts the lattice, as has been observed many times, for example, in cubic crystals of fluorides and oxyfluorides [9–11]. NMR studies of $(\text{NH}_4)_2\text{WO}_2\text{F}_4$ have revealed [8] that the motion of the partially ordered octahedra above 230 K is characterized by dynamic orientation disorder associated with their rotation around the O=W–F axis (the interatomic distances are $d_{\text{W-O}} = 1.737$ Å, $d_{\text{W-F}} = 2.018$ Å).

However, the authors of [8] failed to determine the coordinates of hydrogen atoms. This allowed us to assume that these atoms are disordered in the initial phase and their ordering due to the phase transition can cause a substantial change in entropy.

In order to obtain more reliable information on the number of phase transitions, their thermodynamic properties, the structural changes at the phase transitions, and the temperature–pressure phase diagram, we are currently conducting structural studies of the distorted phases on single-crystal samples and measurements of the heat capacity using the adiabatic-calorimeter and DTA methods under hydrostatic pressure.

ACKNOWLEDGMENTS

This work was supported by the Foundation for Support of National Science, the Russian Foundation for Basic Research (grant no. 03-02-16079), a grant from the president of the Russian Federation (project NSh-939.2003.2), and the Krasnoyarsk Krai Science Foundation (project no. 14G110).

REFERENCES

1. V. S. Sergienko, M. A. Porai-Koshits, and T. S. Khodashova, *Zh. Strukt. Khim.* **13** (3), 461 (1972).

2. M. Vlasse, J. M. Moutou, M. Cervera-Marsal, J.-P. Chaminade, and P. Hagenmuller, *Rev. Chim. Miner.* **19**, 58 (1982).
3. A. M. Srivastava and J. F. Ackerman, *J. Solid State Chem.* **98**, 144 (1992).
4. K. R. Heier, A. J. Norquist, C. G. Wilson, C. L. Stern, and K. R. Poeppelmeier, *Inorg. Chem.* **37**, 76 (1998).
5. K. R. Heier, A. J. Norquist, P. S. Halasyamani, A. Duarte, C. L. Stern, and K. R. Poeppelmeier, *Inorg. Chem.* **38**, 762 (1999).
6. M. E. Welk, A. J. Norquist, C. L. Stern, and K. R. Poeppelmeier, *Inorg. Chem.* **40**, 5479 (2001).
7. P. A. Maggard, A. L. Kopf, C. L. Stern, and K. R. Poeppelmeier, *Inorg. Chem.* **41**, 4852 (2002).
8. N. M. Laptash, A. A. Udovenko, A. B. Slobodyuk, and V. Ya. Kavun, *Abstracts of Papers of the 14th European Symposium on Fluorine Chemistry, Poznan, Poland, 2004* (Poznan, 2004), p. 253.
9. I. N. Flerov, M. V. Gorev, K. S. Aleksandrov, A. Tresaud, J. Grannec, and M. Couzi, *Mater. Sci. Eng.*, **R 24** (3), 81 (1998).
10. A. A. Udovenko, N. M. Laptash, and I. G. Maslennikova, *J. Fluorine Chem.* **124**, 5 (2003).
11. I. N. Flerov, M. V. Gorev, V. D. Fokina, A. F. Bovina, and N. M. Laptash, *Fiz. Tverd. Tela (St. Petersburg)* **46** (5), 888 (2004) [*Phys. Solid State* **46**, 915 (2004)].

Translated by G. Tsydynzhapov